

Extension of the a-Si:H electronic transport model to $\mu\text{-Si:H}$: use of the $\mu^0\tau^0$ product to correlate electronic transport properties and solar cell performances

M. Goerlitzer, P. Torres, C. Droz*, A. Shah

Institute of Microtechnology, University of Neuchatel, Brèguet 2, 2000 Neuchatel, Switzerland

Abstract

The aim of this communication is to show that it is possible to extend the model of the electronic transport developed for amorphous silicon (a-Si:H) to microcrystalline silicon ($\mu\text{-Si:H}$). By describing the electronic transport with the $\mu^0\tau^R$ products (mobility \times recombination time) as a function of the Fermi level, we observed the same behaviour for both materials, indicating a similar type of recombination. Moreover, applying the normalised $\mu^0\tau^0$ product (mobility \times life-time) obtained by combining the photoconductivity (σ_{photo}) and the ambipolar diffusion length (L_{amb}) measured in individual layers, we are able, as in the case of a-Si:H, to predict the quality of the solar cells incorporating these layers as the active $\langle i \rangle$ layer.

Keywords: Microcrystalline silicon; Photoconductivity; Ambipolar diffusion length

1. Introduction

In comparison with the encouraging results already obtained in practice for solar cells made of hydrogenated microcrystalline silicon ($\mu\text{-Si:H}$) [1,2], very little is known so far about the electrical transport properties of this material. However, a possibility to predict the limitation of collection in p-i-n (or n-i-p) solar cells from

* Corresponding author.

E-mail address: corinne.droz@imt.unine.ch (C. Droz)

the “quality” of electronic transport as measured on individual $\langle i \rangle$ layers would be of great interest.

The relevant transport parameters in p-i-n solar cells are the mobility μ and the recombination time τ^R : for a given electric field E , the $\mu\tau^R$ product is proportional to the average distance d which is covered by a free carrier before being lost by recombination ($d = \mu\tau^R E$). This characteristic distance can directly be related to the possible thickness of the $\langle i \rangle$ layer (taking into account the built-in potential) which still allows the collection of the photogenerated carriers. Because $\mu\text{-Si:H}$ as well as a-Si:H solar cells are of the p-i-n form, for both types of material the relevant parameters for the electronic transport are these $\mu\tau^R$ products.

In layers, the photoconductivity gives access to the $\mu\tau^R$ product of the majority carriers, here the electrons ($\sigma_{\text{photo}} \propto \mu_n^0 \tau_n^R$), and the ambipolar diffusion length [3,4] to the $\mu\tau^R$ product of minority carriers, here the holes ($L_{\text{amb}} \propto \mu_p^0 \tau_p^R$). For $\mu\text{-Si:H}$, we showed that it is still correct to measure L_{amb} with the grating method [5,6]. However, our first attempt to correlate the $\mu\tau^R$ products with the defect density, the structure (crystallinity and/or crystallographic orientation) or the density of oxygen (residual [7] or due to post-oxidation [8]) failed. The idea was therefore to take the Fermi level (E_f) to monitor the $\mu\tau^R$ products. Instead of explicitly using E_f , we use the parameter b defined by us as $b = \mu_n^0 n_f / \mu_p^0 p_f$, with n_f, p_f the density of the photogenerated free electrons, and holes, respectively [9]. In fact, b can be easily evaluated from the measured values of σ_{photo} and L_{amb} (as shown in [10]), whereas the Fermi level would require separate measurements. b describes the Fermi level also in the case of $\mu\text{-Si:H}$ as demonstrated in Ref. [5]: for E_f at midgap, $b \approx 1$; for n-type samples $b > 1$ and increases as E_f moves upward from midgap.

We will show here that by representing for $\mu\text{-Si:H}$ the measured $\mu\tau^R$ products as a function of b we obtain a similar graph as for a-Si:H. Thus, we conjecture that the electronic transport model developed for a-Si:H (see for example, Ref. [11]) is also applicable to $\mu\text{-Si:H}$. In this case we can use the parameter $\mu^0 \tau^0$ introduced for a-Si:H [12] to describe the “electronic quality” of $\mu\text{-Si:H}$ layers. $\mu^0 \tau^0$ is a normalised $\mu\tau^R$ product, assuming that all the defects are neutral (D^0 states), and permits one to predict the collection in a solar cell from the quality of the electronic transport measured in an individual $\langle i \rangle$ layer.

2. Experimental

The films studied in this communication were grown by the VHF-GD deposition technique [13]. To obtain nearly intrinsic $\mu\text{-Si:H}$ (Fermi level near midgap), a gas purifier was used [7]. Two series were deposited at a fixed plasma excitation frequency of 130 MHz, fixed effective deposition temperature of 220°C and fixed pressure of 0.8 mbar. For the first series (series no. 1) the dilution of silane by hydrogen ($[\text{SiH}_4]/([\text{SiH}_4] + [\text{H}_2])$) was kept constant at 5%, while for the second one (series no. 2) the dilution was kept constant at 7.5%. The electrode area was 139 cm². The only parameter varied was the VHF-power, as measured just before the matching network. The value of VHF-power ranged between 9 and 30 W for series no. 1, and

between 30 and 70 W for series no. 2. Specific details of the reactor can be found elsewhere [13,14]. The thickness of the films ranged between 2.1 and 2.8 μm for series no. 1, and between 1.6 and 2.5 μm for series no. 2. The films were deposited on AF45 (Schott) glass for the coplanar measurements, with aluminium contacts (gap 0.5 mm). We used a Krypton laser (647 nm) to measure σ_{photo} and L_{amb} . The second series (series no. 2) was also incorporated into solar cells as the active intrinsic layer. More details on deposition conditions of series no. 1 can be found in [14], while those for series no. 2 and the corresponding solar cell fabrication conditions as well as the measurement techniques for these solar cells are described in [15].

3. Results and discussion

As stated in the introduction, we measured σ_{photo} and L_{amb} for the two power series in order to have access to the $\mu\tau^R$ products. Fig. 1 represents the results in function of the VHF-power used for the deposition. From X-ray diffraction, we know that these two series are clearly microcrystalline. The first one (series no. 1) has an “ideal” preferential crystallographic orientation in the $\langle 2\ 2\ 0 \rangle$ direction (perpendicular to the substrate), and shows surprisingly no $\langle 1\ 1\ 1 \rangle$ diffraction peak at all. This is evaluated by comparing the ratio $\langle 2\ 2\ 0 \rangle / \langle 1\ 1\ 1 \rangle$ in our samples with the same ratio in a silicon powder, NBS no. 640. This “ideal” preferential orientation remains the same for all the samples (i.e. for all values of VHF-power). The defect density for this series increases by a factor of ten with VHF-power, whereas the density of oxygen remains constant ($\approx 3 \times 10^{18}$ atoms/cm³). The details of these measurements are described elsewhere [8]. The second one (series no. 2) shows also a preferential crystallographic orientation in the $\langle 2\ 2\ 0 \rangle$ direction, but less “ideal”, as $\langle 1\ 1\ 1 \rangle$ peaks are present for the

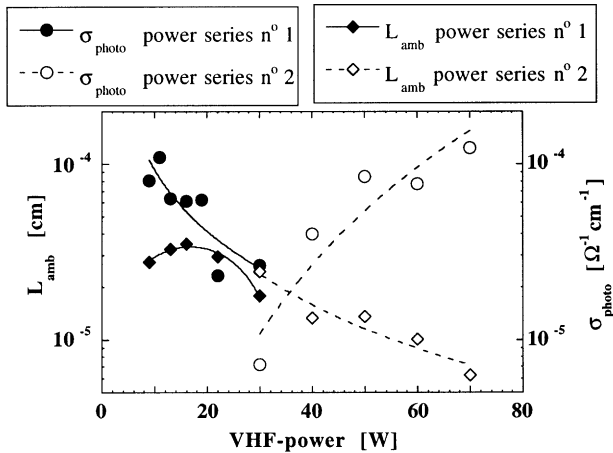


Fig. 1. σ_{photo} and L_{amb} for the two power series (see text) as a function of the VHF-power of deposition. The electrode area was 139 cm². The generation rate used for the measurements is 1.5×10^{20} cm⁻³s⁻¹. The lines are only to guide the eyes.

samples of this series. Moreover, this preferential orientation varies with the power, showing a maximum of the ratio $\langle 220 \rangle / \langle 111 \rangle$ around 50 W. For this series the defect density increases with VHF-power by a factor of four, whereas the oxygen density grows from 3×10^{19} to 2×10^{20} atoms/cm³. Here again the details of these measurements can be found in Ref. [15]. The question is now what is the link between these observations and the electronic transport parameters σ_{photo} and L_{amb} shown in Fig. 1. It can indeed be seen here that neither σ_{photo} nor L_{amb} depend only on defect density or on structure. For series no. 1, the increase of defect density with VHF-power could indeed explain the decrease of σ_{photo} , but it cannot explain the maximum that is observed in the curve for L_{amb} . As the orientation as well as the oxygen concentration remain constant when VHF-power is increased, we could not, at this point, explain the results. For series no. 2, the increase of the oxygen density could explain the increase of σ_{photo} (oxygen is an n-type dopant), and the increase of defect density could explain the decrease of L_{amb} , but we would have in this case two independent explanations for the same samples, and this does not constitute a satisfactory situation.

As individually neither the structure, nor the defect density, nor the oxygen concentration could explain the transport measurements, we decided to use the Fermi level, monitored by the parameter b as the discriminating parameter. In Fig. 2 we see that with this representation, the data that looked quite confusing in Fig. 1 now takes

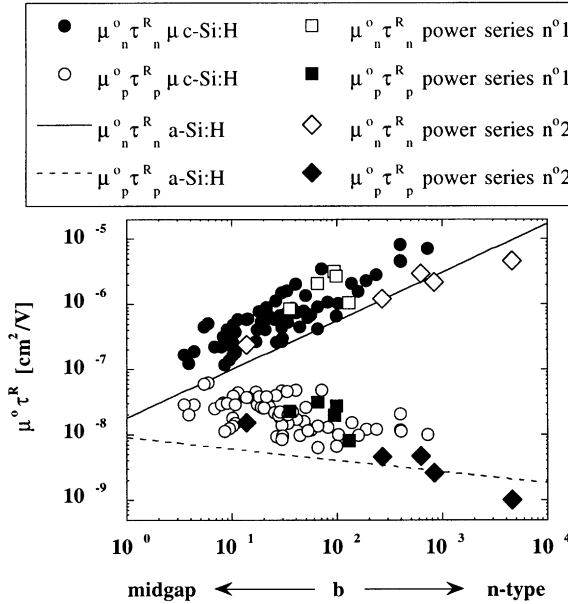


Fig. 2. $\mu^0\tau^0$ products for the two power series (see text), as well as $\mu^0\tau^0$ products for all our $\mu\text{c-Si:H}$ samples for all the experimental conditions (all markers) [6], as a function of the Fermi level monitored by the parameter $b = \mu_n^0 n_t / \mu_p^0 p_t$. In comparison, the mean values obtained in the case of a-Si:H as measured by Sauvain [16].

on a very regular form. An anti-correlation between the $\mu\tau^R$ values of the minority carriers and that of the majority carriers can be identified: this is a behaviour that is similar to what is observed in a-Si:H. This anti-correlation is predicted by our electronic transport model for a-Si:H [10,11], when taking into account the three states of charge of the dangling bonds (deep defects) and their functions of occupation.

In order to see if it is reasonable to extend the use of the model developed for a-Si:H also to $\mu\text{c-Si:H}$, we have represented all the measured values of $\mu\tau^R$, for all the samples we have observed and for all experimental conditions [6]. Fig. 2 shows the results, in comparison with the mean values obtained in the case of a-Si:H [16]. This figure confirms that the model is certainly a reasonable approximation also for the case of $\mu\text{c-Si:H}$. Fig. 2 supports our previous observations [8] that electronic transport in $\mu\text{c-Si:H}$ is on an average slightly better than in a-Si:H.

Up to now we did not have to introduce a specific model for recombination in order to evaluate the $\mu\tau^R$ or the parameter b . But at this point, as we have seen that the electronic transport model fits measurement, we go one step ahead: assuming that the recombination process is the same in $\mu\text{c-Si:H}$ as in a-Si:H, we introduce the quality parameter $\mu^0\tau^0$, defined for a-Si:H [12] as a normalised $\mu\tau^R$ product which does not depend on the experimental conditions (i.e. on the Fermi level) and which is used to predict the efficiencies of solar cells, as far as the cell performance is limited by the $\langle i \rangle$ layer. Fig. 3 represents, for our power series no. 2 of $\mu\text{c-Si:H}$ layers, the values of the $\mu^0\tau^0$ product compared with the efficiencies of n-i-p solar cells incorporating such layers as the active $\langle i \rangle$ layer. Globally, the correlation is successful and indicates the opportunity of using the $\mu^0\tau^0$ quality parameter for $\mu\text{c-Si:H}$ also. We have to note that a correlation between layer properties and solar cell efficiencies can obviously be expected only when the latter is governed by the quality of the intrinsic layer and not by other factors like interface problems. However, we have to state here that so far only a single series of layers and cells have been evaluated; to fully justify the use of the $\mu^0\tau^0$ product in the case of $\mu\text{c-Si:H}$ layers and cells, additional work is needed.

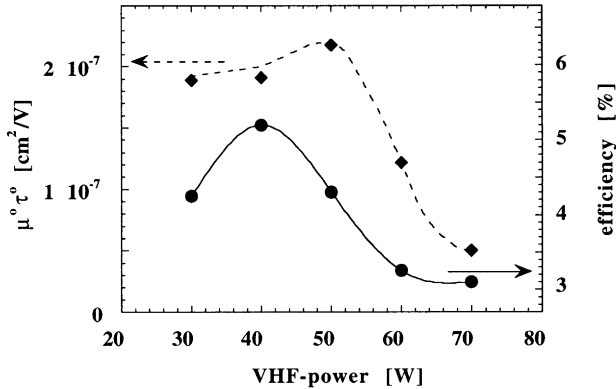


Fig. 3. $\mu^0\tau^0$ products, which measure the quality of the material, evaluated in the same manner as for a-Si:H, and solar cell efficiencies [12,15] incorporating the same material as the active $\langle i \rangle$ layer. The lines are only to guide the eyes.

4. Conclusions

We observed for $\mu\text{-Si:H}$ that it is not possible to correlate individually the electrical transport properties with the structure, the defect density or the oxygen contamination when the measured parameters are the mobility \times recombination time ($\mu\tau^{\text{R}}$) products. However, if the $\mu\tau^{\text{R}}$ products are represented as a function of the Fermi level (via a certain parameter b which varies proportionally to the ratio $n_{\text{f}}/p_{\text{f}}$ of the free carrier densities), a clearer picture results: the behaviour of the $\mu\tau^{\text{R}}$ products for the majority carriers can be seen to be anti-correlated with the $\mu\tau^{\text{R}}$ products for the minority carriers, as already observed for a-Si:H. This justifies the use of the recombination model developed for a-Si:H also for $\mu\text{-Si:H}$ layers. This has a specific consequence: we can now use, also for $\mu\text{-Si:H}$, the normalised $\mu^0\tau^0$ products as measured in individual $\langle i \rangle$ layers, to predict the performances of solar cell incorporating the same layer as the active $\langle i \rangle$ layer.

Acknowledgements

This work was supported by the Swiss National Science Foundation under FN-45696 and by the Swiss Federal Office of Energy under Research Grant 19431.

References

- [1] J. Meier, P. Torres, R. Platz, S. Dubail, U. Kroll, J.A. Anna Selvan, N. Pellaton Vaucher, Ch. Hof, D. Fischer, H. Keppner, A. Shah, K.-D. Ufert, P. Giannoulès, J. Koehler, Mater. Res. Soc. Symp. Proc. 420 (1996) 3.
- [2] J. Meier, S. Dubail, J. Cuperus, U. Kroll, R. Platz, P. Torres, J.A. Anna Selvan, P. Pernet, N. Beck, N. Pellaton Vaucher, Ch. Hof, D. Fischer, H. Keppner, A. Shah, Proceedings of the 17th ICAMS, Budapest (1997), Special Edition of J. Non-Cryst. Solids 227–230 (1998) 1250.
- [3] D. Ritter, K. Weiser, E. Zeldov, J. Appl. Phys. 62 (1987) 4563.
- [4] I. Balberg, Mater. Res. Soc. Symp. Proc. 258 (1992) 693.
- [5] M. Goerlitzer, N. Beck, P. Torres, J. Meier, N. Wyrsh, A. Shah, J. Appl. Phys. 80 (1996) 5111.
- [6] M. Goerlitzer, Ph.D. Thesis, University of Neuchâtel, 1998, ISBN 2-9700197-0-1.
- [7] P. Torres, J. Meier, R. Flückiger, U. Kroll, J.A. Anna Selvan, H. Keppner, A. Shah, S.D. Littelwood, I.E. Kelly, P. Giannoulès, Appl. Phys. Lett. 69 (1996) 1373.
- [8] M. Goerlitzer, P. Torres, N. Beck, N. Wyrsh, H. Keppner, J. Pohl and A. Shah, Proceedings of the 17th ICAMS, Budapest (1997), Special Edition of J. Non-Cryst. Solids 227–230 (1998) 996.
- [9] A. Shah, E. Sauvain, J. Hubin, P. Pipoz, C. Hof, Philos. Mag. B 75 (1997) 925.
- [10] P. Pipoz, E. Sauvain, J. Hubin, A. Shah, Mater. Res. Soc. Symp. Proc. 258 (1992) 777.
- [11] J. Hubin, A. Shah, E. Sauvain, P. Pipoz, J. Appl. Phys. 78 (1995) 6050.
- [12] N. Beck, N. Wyrsh, Ch. Hof, A. Shah, J. Appl. Phys. 79 (1996) 9361.
- [13] H. Curtins, N. Wyrsh, M. Favre, A. Shah, Plasma Chem. and Plasma Proc. 7 (1987) 267.
- [14] P. Torres, Ph.D. Thesis, University of Neuchâtel, 1998, ISBN 3-930803-51-8.
- [15] P. Torres, J. Meier, U. Kroll, N. Beck, H. Keppner, A. Shah, 26th IEEE Photovoltaic Specialists Conference, Anaheim, CA, 1997, p. 711.
- [16] E. Sauvain, Ph.D. Thesis, University of Neuchâtel, 1992.